INFORMATION
Volume 28. Number 1, pp.5-21
ISSN 1343-4500 eISSN 1344-8994

Polytope Typology A: The separation of facial polytopes in the morphology of the regular and semi-regular polyhedra and tessellations

Robert C. Meurant

Director, Institute of Traditional Studies; Adjunct Professor, Seoul National University PG College of Eng.; Exec. Director, Research and Education, Harrisco Enco • rmeurant@gmail.com • http://www.rmeurant.com/its/

Abstract

Inspired by Critchlow [1], and Grünbaum and Shephard [2], previous work has proposed an integral 2.5D cubic schema of the regular and semi-regular polyhedra and polygonal tessellations of the plane for each class of symmetry. This schema is differentiated into an upper and lower layer of 4 polytopes each, and characterized by corresponding pairs of upper and lower polytopes [3]. The motif of paired two-step sequences of first alternating separation and morphological transformation of faces, and second morphological transformation and separation of faces is explored, which in 2D consideration of the 2.5D schema are disposed about the vertical axis, as characterized by the correspondence between the *PPs* of the lower and upper squares (rhombi).

Developing earlier sustained research [3−11], this paper addresses a deeper typology of morphological transformation of the primary polytopes, involving the separation of one gendered set of the negative (–ve), neutral (ntrl), or positive (+ve) facial polytopes along the Y, Z, and X axes of the cubic schema. While one set of faces separates, the other two sets morph or project through null→regular or quasi-regular→double facial levels (0→α|β→2) of the rhombic schema or its reflection. Each facial set only separates once, faces separating by d=0→1. The cubic schema exhibits significant three-fold symmetry by gender. The separation of faces schema adequately describes the morphology of the three classes of regular and semi-regular polyhedra of {2,3,3}, {2,3,4}, and {2,3,5} symmetry, and the two classes of polygonal tessellations of {2,3,6} and {2,4,4} symmetry.

Key words: morphology, polyhedra, separation of faces, tessellations

1. Class II and generic pairing of polyhedra by the separation of faces

Figure 1 of the 2.5D schema shows that the pairings of polyhedra within any one class can be characterized by the separation of one set of the negative, neutral, or positive surface polytopes on the (left to right) Y, Z, or X axes, respectively. Three significant kinds of pairings of *PP*s are evident in the 2.5D schema, one for each orthogonal axis. These are described for Class II of {2,3,4} symmetry, which is characterized by the −ve, neutral, and +ve axes of the class, and thus of each of its individual polytopes, being the √1, √2, and √3 (100, 110, 111) axes, respectively, of the cube.

In this class of 3D polyhedra, the +ve and −ve polar polytopes assume different (dual) forms; this contrasts with Class I also of 3D polyhedra, in which the two polar polytopes take the same tetrahedral form, though in alternative orientation, or Class V of 2D polygons, in which both polar polytopes assume the same form of the square, but in different location. The symmetry axes in the other classes are not in general orthogonal; meanwhile, Class II precisely consists of the *PP*s of the Class III honeycombs, corresponding to the primary components of the Class III honeycomb periodic all-space-filling arrays. Later comparison of Classes II and IV illustrates the differences between 3D polyhedral and 2D polygonal form, while considering classes with different polar polytopes, as opposed to having the same, though reoriented (3D) or relocated (2D) form. The beautiful integrity of interrelationship is clearly revealed in Fig. 1:

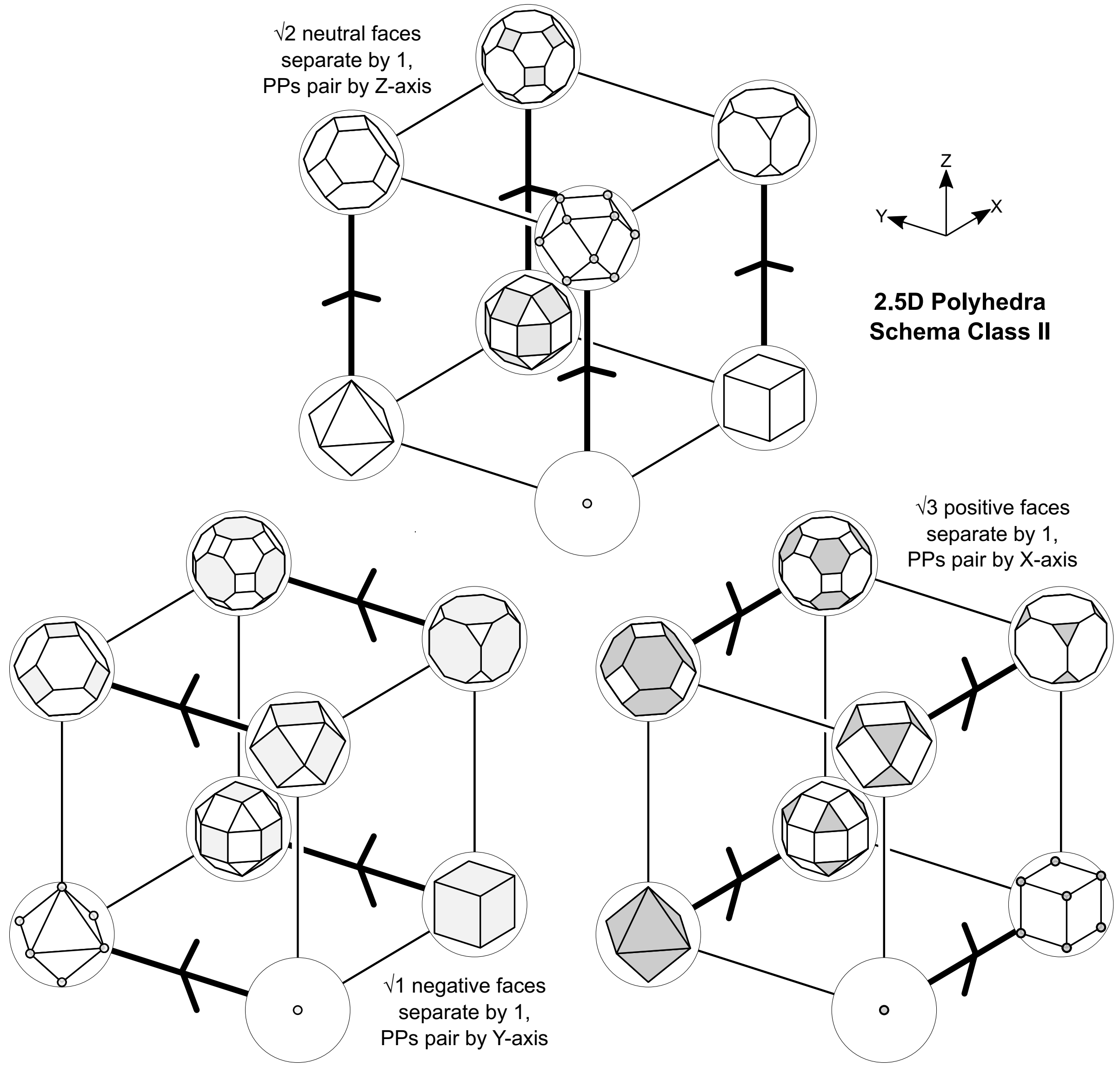

Fig. 1: Pairings of the Class II polyhedra according to −ve (left), neutral (upper), or +ve (right) faces, which separate from *adjoining* (sharing a V or E) to *adjacent* by distance unit 1 = edge length. CB and OH are considered the −ve and +ve polar polytopes, respectively, with facial PTs shown as −ve (light grey) and +ve (dark grey), respectively, while neutral polytopes are shown in mid-grey, or as thick black edge.

Table I. Separating PP pairs for Class II and their source and goal polytopes.

Negative			Neutral			Positive		
Separating facial PTs	Source polytope	Goal polytope	Separating facial PTs	Source polytope	Goal polytope	Separating facial PTs	Source polytope	Goal polytope
V^-	VP_2	OH	V^0	VP_2	CO	V^+	VP_2	CB
SQ^-	CB	$SRCO$	E^0_α	OH	TO	TR^+	OH	$SRCO$
RS^-	CO	TO	E^0_β	CB	TC	RT^+	CO	TC
OG^-	TC	$GRCO$	SQ^0	$SRCO$	$GRCO$	HX^+	TO	$GRCO$

N.B. This paper modifies my previous conventions: Vertex $VT \rightarrow V$; neutral vertex $NV \rightarrow V^0$; edge $EG \rightarrow E$, neutral edge $NE \rightarrow E^0$; neutral square $NS \rightarrow SQ^0$; Facial polytope → F; on-axis 0D V^0 (the 1-gon, of 1 E and 1 V`) and 1D E^0 (the 2-gon, of 2 E and 2 V^0), and 2D polygons (TR, HX, SQ, …), are considered F (Facial PTs; kindly refer to Nomenclature at end of paper).

The Y-axis of the schema (rising leftwards), shows the separation of *negative* faces (light grey; lower left), as adjoining (coincident) V^{-}s of the VP separate to adjacent V^{-}s of the OH (its nodes); adjoining SQ^{-}s of the CB separate to adjacent SQ^{-}s of the $SRCO$; adjoining RS^{-}s of the CO separate to adjacent RS^{-}s of the TO; and adjoining OG^{-}s of the TC separate to adjacent OG^{-}s of the $GRCO$. In each case, *adjoining* pairs of negative polytopes of a PP that share a V^{0} or E^{0} separate by edge length unit distance 1 to become *adjacent* negative polytopes of its PP pair.

The Z-axis of the schema (rising vertically) shows the separation of *neutral* faces (mid-grey; upper), as adjoining (coincident) V^{0}s of the VP separate to adjacent V^{0}s of the CO (its nodes); adjoining E^{0}s of the OH separate to adjacent E^{0}s of the TO; adjoining E^{0}s of the CB separate to adjacent E^{0}s of the TC; and adjoining SQ^{0}s of the $SRCO$ separate to adjacent SQ^{0}s of the $GRCO$. In each case, adjoining pairs of neutral surface polytopes of a PP, sharing a V or E that need not be +/0/−ve, e.g., of $SRCO$, separate by d=1 to become adjacent neutral Fs of its PP pair.

The X-axis of the schema (rising rightwards) shows the separation of *positive* faces (dark grey; lower right), as adjoining (coincident) V^{+}s of the VP separate to adjacent V^{+}s of the CB (its nodes); adjoining TR^{+}s of the OH separate to adjacent TR^{+}s of the $SRCO$; adjoining RT^{+}s of the CO separate to adjacent RT^{+}s of the TC; and adjoining HX^{+}s of the TO separate to adjacent HX^{+}s of the $GRCO$. In each case, adjoining pairs of positive polytopes of a PP, sharing a V^{0} or E^{0}, separate by distance 1 to become adjacent positive polytopes of its PP pair.

Figure 2 combines these various correspondences by the separation of facial polytopes by unit distance into the one illustration (Fig. 2), with the exemplary Class II shown at left and middle, and all classes (generic) at right. In each case of facial separation, *adjoining* pairs of polytopes of a PP (d=0) separate by unit distance d=1 (= length of polytope side) to become *adjacent* polytopes of its PP pair:

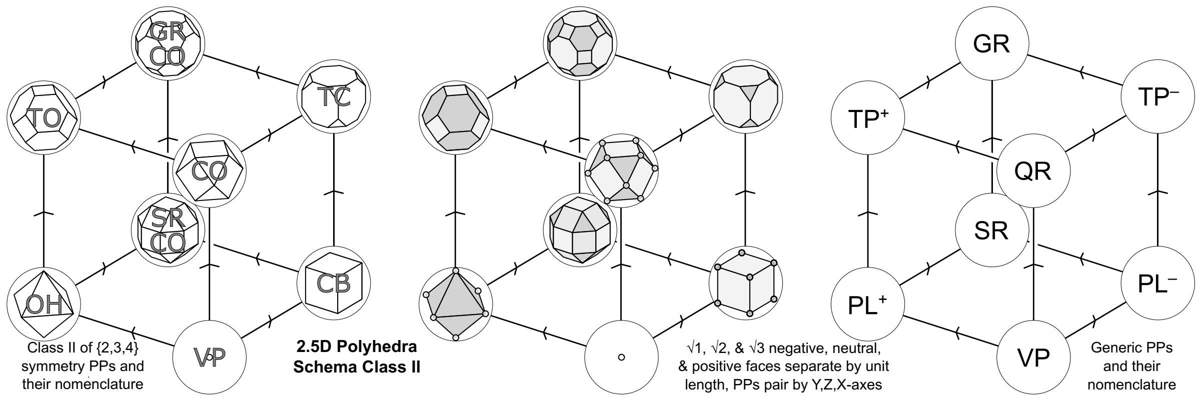

Fig. 2: Class II (left and middle), and generic (all classes; right) paired correspondences of *PP*s.

2. The Class II associated evolution of non-separating morphing faces

As my earlier papers have partially explored [3, 4] and developing the description in the previous section, as one set of faces separates, the other 2 sets of faces evolve, doing so consistently according to a rhombic schema; refer Fig. 3 and Table III.

Negative Separations: On the Y-axis of the cubic schema rising leftwards, as the −ve faces (light grey) separate, the +ve faces expand, evolving according to the rhombic schema of Fig. 3c from level 0 or 1 to the next higher level (1 or 2). Meanwhile, the neutral faces project (extrude), evolving to an analogous rhombic schema from level 0 or 1 to the next higher level (1 or 2; Fig. 3b). Figure 1 (lower left) shows that in Class II, as (lower rhomb) V^{-}s and SQ^{-}s separate, V^{+}s expand to TR^{+}s; while (upper rhomb) as RS^{-}s and OG^{-}s separate, RT^{+}s expand to HX^{+}s, while the V^{0}s and E_{β}s of the lower and upper rhombs project to E_{α}s and SQ^{0}s, respectively (Fig. 1, lower left).

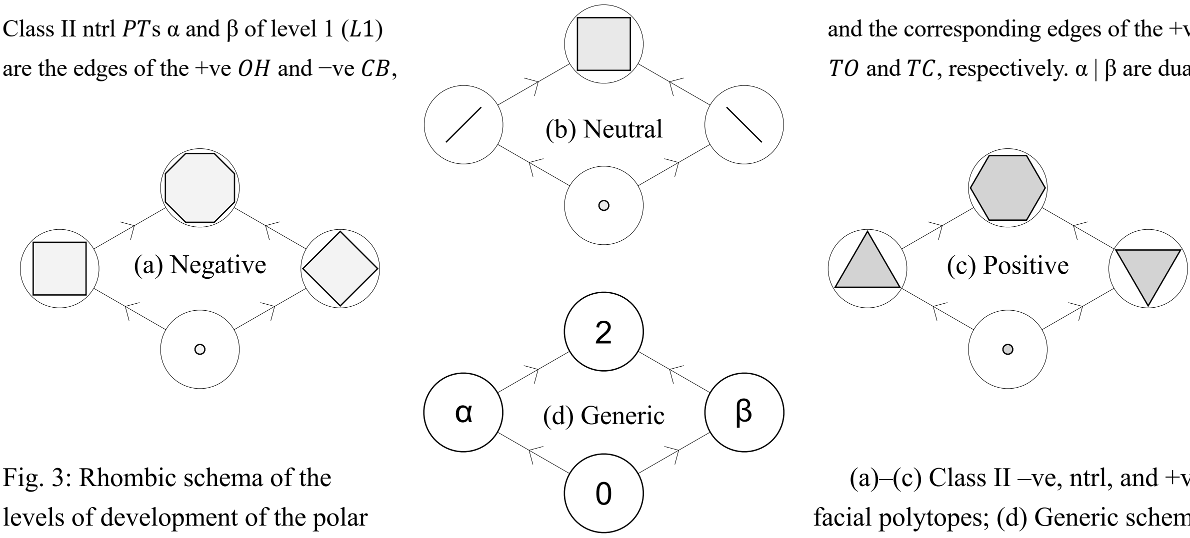

Class II ntrl PTs α and β of level 1 ($L1$) are the edges of the +ve OH and −ve CB, and the corresponding edges of the +ve TO and TC, respectively. α | β are dual.

Fig. 3: Rhombic schema of the levels of development of the polar facial polytopes: (a)–(c) Class II –ve, ntrl, and +ve facial polytopes; (d) Generic schema of Classes I–V, with levels $L0$−$L2$.

Neutral Separations: On the Z-axis of the cubic schema rising vertically, as the neutral faces (mid-grey) separate, both the +ve and the −ve faces expand, evolving according to the rhombic schema from level 0 or 1 to the next higher level (1 or 2; Fig. 3d). In Class II, as the V^0s and E^0_βs separate, V^+s morph to RT^+s; and as (back left rhomb) E^0_αs and SQ^0s of the front right rhomb separate, TR^+s morph to HX^+s. As the V^0s and E^0_αs of the front left rhomb separate, V^-s morph to RS^-s; and as the E^0_βs and SQ^0s of the back right rhomb separate, SQ^-s morph to OG^-s (Fig. 1, upper middle).

Positive Separations: On the X-axis of the schema rising rightwards, as the +ve faces separate, the −ve faces expand, evolving according to the rhombic schema from levels 0 or 1 to the next higher level (1 or 2; Fig. 3a). Meanwhile, the neutral faces project (extrude), evolving according to the analogous rhombic schema from level 0 or 1 to the next higher level (1 or 2; Fig. 3b). In Class II, as the V^+s and TR^+s of the lower rhomb separate, V^-s expand to SQ^-s; while as the RT^+s and HX^+s of the upper rhomb separate, RS^-s expand to OG^-s; meanwhile, the V^0s and E^0_αs of the lower and upper rhombs extrude to E^0_βs and SQ^0s, respectively (Fig. 1, lower right).

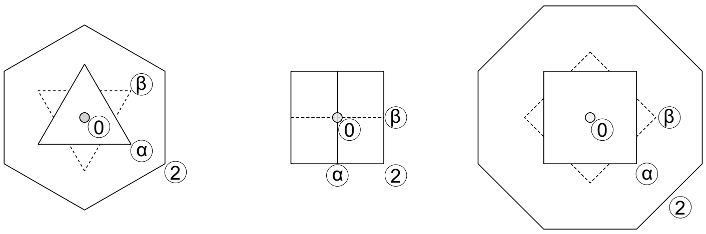

Fig. 4: On-axis Class II null, regular and quasi-regular (dashed), and double (frequency) (0, α and β, 2) faces from center VT (circle) outwards and front to back for (left to right): +ve, ntrl, and −ve axes, where null (0) refers to the 0D case; regular (α) to the same orientation face as for the regular PLs (OH, CB), and quasi-regular (β) as for the quasi-regular QR (CO); and double (2) to the 2-frequency face. For neutrals, α and β faces are defined as the 2-gon E^0s of the +ve and −ve PLs OH and CB, respectively.

The neutral faces (2-gon neutral edges of the PP) that are generated at the middle Level 1 $L1$) of the facial rhombic schema shown in Fig. 3 are of two kinds of orientations, α and β, depending on whether they characterize the +ve or −ve PLs (in Class II, OH and CB), respectively. This is analogous to the central $L1$ distinction of the +ve and −ve faces into α | β orientations (Figs. 3b and 4). The morphology of this α | β neutral dichotomy analogues that of the two kinds of neutral polyhedra of the Class III honeycombs, particularly in the primary and tertiary arrays [5−11], where the neutral diverges into complementary pairs.

Table II. Generic Schema of the 5 Classes of the Regular and Semi-regular Polyhedra and Tessellations.

Polytope Class	Symmetry {0,+,−}	Lower Rhomb				Upper Rhomb			
		VP	P^+	P^-	SR	QR	$TrncP^+$	$TrncP^-$	GR
I	{2,3,3}	VP_I	TH^+	TH^-	$SR\ TH{:}TH$	$TH{:}TH$	TT^+	TT^-	$GR\ TH{:}TH$
II	{2,3,4}	VP_{II}	OH^+	CB^-	$SR\ OH{:}CB$	$OH{:}CB$	TO^+	TC^-	$GR\ OH{:}CB$
III	{2,3,5}	VP_{III}	IC^+	DC^-	$SR\ IC{:}DC$	$IC{:}DC$	TI^+	TD^-	$GR\ IC{:}DC$
IV	{2,3,6}	VP_{IV}	TR^+	HX^-	$SR\ TR{:}HX$	$TR{:}HX$	RT^+	RH^-	$GR\ TR{:}HX$
V	{2,4,4}	VP_V	SQ^+	SQ^-	$SR\ SQ{:}SQ$	$SQ{:}SQ$	RS^+	SQ^-	$GR\ SQ{:}SQ$

Table III. Class II Separation of one set of (−ve, ntrl, or +ve) facial pairs of PPs with their associated morphological changes of the other two sets of facial polytopes from source to goal ($OH{:}CB = CO$).

Separating facial PTs	Primary Polytope (PP) transition	Source facial PTs	Goal facial PTs	Source facial PTs	Goal facial PTs
Negative facial PT separation		Neutral facial PT projection		Positive facial PT expansion	
V^-	$VP_2 \rightarrow OH$	${}_0V^0$	${}_0E^0_\alpha$	${}_0V^+$	${}_0TR^+$
SQ^-	$CB \rightarrow SRCO$	${}_0E^0_\beta$	${}_0SQ^0$	${}_1V^+$	${}_1TR^+$
RS^-	$CO \rightarrow TO$	${}_1V^0$	${}_1E^0_\alpha$	${}_0RT^+$	${}_0HX^+$
OG^-	$TC \rightarrow GRCO$	${}_1E^0_\beta$	${}_1SQ^0$	${}_1RT^+$	${}_1HX^+$
Neutral facial PT separation		Positive facial PT expansion		Negative facial PT expansion	
V^0	$VP_2 \rightarrow CO$	${}_0V^+$	${}_0RT^+$	${}_0V^-$	${}_0RS^-$
E^0_α	$OH \rightarrow TO$	${}_0TR^+$	${}_0HX^+$	${}_1V^-$	${}_1RS^-$
E^0_β	$CB \rightarrow TC$	${}_1V^+$	${}_1RT^+$	${}_0SQ^-$	${}_0OG^-$
SQ^0	$SRCO \rightarrow GRCO$	${}_1TR^+$	${}_1HX^+$	${}_1SQ^-$	${}_1OG^-$
Positive facial PT separation		Negative facial PT expansion		Neutral facial PT projection	
V^+	$VP_2 \rightarrow CB$	${}_0V^-$	${}_0SQ^-$	${}_0V^0$	${}_0E^0_\beta$
TR^+	$OH \rightarrow SRCO$	${}_1V^-$	${}_1SQ^-$	${}_0E^0_\alpha$	${}_0SQ^0$
RT^+	$CO \rightarrow TC$	${}_0RS^-$	${}_0OG^-$	${}_1V^0$	${}_1E^0_\beta$
HX^+	$TO \rightarrow GRCO$	${}_1RS^-$	${}_1OG^-$	${}_1E^0_\alpha$	${}_1SQ^0$

3. Class IV pairing of polygonal arrays by the separation of faces

Class IV of the regular and semiregular polytopes comprises the *Tri−Hex* arrays, in which the polar PTs are the +ve triangular and −ve hexagonal regular tessellations. Class IV is similarly characterized to Class II, even though it differs in dimension, in being of 2D tessellations, rather than 3D polyhedra; unlike the other 2D Class V of the $SQ{-}SQ$ cluster of arrays, its polar elements assume different geometric form (Fig. 5, upper right).

Negative Separations: On the Y-axis of the cubic schema rising leftwards, as the V^-s and HX^-s of the lower rhomb separate, V^+s expand to TR^+s; while as the RH^-s and DD^-s of the upper rhomb separate, RT^+s expand to HX^+s; and meanwhile, the V^0s and E_βs of the lower and upper rhombs project to E_αs and SQ^0s, respectively (Fig. 5, lower left).

Neutral Separations: On the Z-axis of the cubic schema rising vertically, as the V^0s and E^0_βs of the front right rhomb separate, V^+s morph to RT^+s; as the E^0_αs and SQ^0s of the back left rhomb separate, TR^+s morph to HX^+s. As the V^0s and E^0_αs of the front left rhomb separate, V^-s morph to RH^-s; and as the E^0_βs and SQ^0s of the upper right rhomb separate, HX^-s morph to DD^-s (Fig. 5 upper mid-left).

Positive Separations: On the X-axis of the cubic schema rising rightwards, as the V^+s and TR^+s of the lower rhomb separate, V^-s expand to HX^-s; while as the RT^+s and HX^+s of the upper rhomb separate, RH^-s expand to DD^-s; meanwhile, the V^0s and E^0_αs of the lower and upper rhombs extrude to E_βs and SQ^0s, respectively (Fig. 5, lower mid-right).

Upper Rhombus:
Great Rhombic Tri−Hex Array (top)
Truncated Triangular Array and
Truncated Hexagonal Array
(upper left and right)
Quasi-Regular TriHex array (lower)

Lower Rhombus:
Small Rhombic Tri−Hex array (upper)
Triangular Array and Hexagonal Array
(lower left and right)
Verticial Array
(bottom).

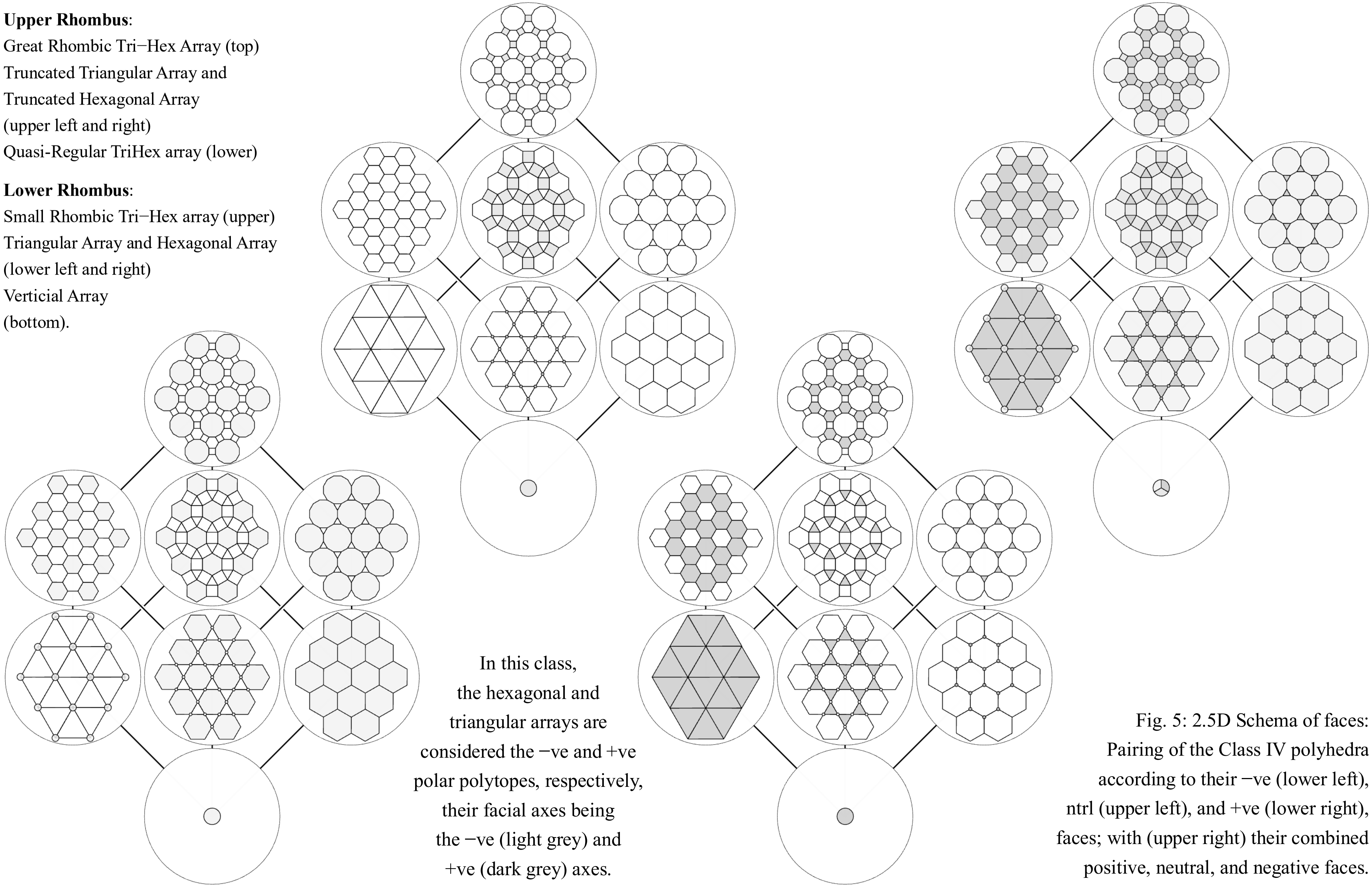

In this class,
the hexagonal and
triangular arrays are
considered the −ve and +ve
polar polytopes, respectively,
their facial axes being
the −ve (light grey) and
+ve (dark grey) axes.

Fig. 5: 2.5D Schema of faces:
Pairing of the Class IV polyhedra
according to their −ve (lower left),
ntrl (upper left), and +ve (lower right),
faces; with (upper right) their combined
positive, neutral, and negative faces.

4. The unfolding of apparent three-fold symmetry

In previous work [3], I exploited the 2D characteristics of the 2.5D schema, integrating the vertical dimension, and associated separation of PP elements into +ve (left; $OH-TO$), neutral (middle; $VP-CO-SRCO-GRCO$), and −ve (right; $CB-TC$). I partially exploited the 3D characteristics of the schema, differentiating the schema primarily into lower (VP, OH, CB, $SRCO$) and upper (CO, TO, TC, $GRCO$) rhombi (top and bottom faces of the cubic schema). Generically, this represents separation into positive $TP^{+}-PL^{+}$, neutral $VP-QR-SR-GR$, and negative $PL^{-}-TP^{-}$, with lower (VP, PL^{+}, PL^{-}, SR) and upper (QR, TP^{+}, TP^{-}, GR) rhombi.

This paper develops these 3D characteristics more fully, considering the √3 long diagonal VP—$GRCO$ to be the primary axis, situated vertically, so the cubic schema can be regarded as a cube balanced on one vertex (VP) (Fig. 6, left), hence emphasizing its 3-fold symmetry: rather than considering +ve and −ve as polar opposites with neutral as central mediating case, the three gender cases of +ve, neutral, and −ve are allowed a degree of equal status, the main distinction being that the neutral faces (2-gon neutral edges of the PP) that are generated at Level 1 of the facial hierarchy are, as before, of two orientations, α and β.

Contemplating the cubic schema in a true 3D multi-axial (microgravitational) sense, any PP enjoys various kinds of pairing relationship with 3 adjoining PPs, 3 distant PPs, and 1 opposite PP; e.g., in Class II, OH—TC, i.e., OH; SR, VP, TO; CO, GR, CB; TC. The most significant of these axial pairs is the primary VP—$GRCO$ √3 axis, as the VP progresses step-wise through its 3 neighboring PPs, OH, CO, CB; its 3 more distant relatives, TC, $SRCO$, TO; to culminate in its opposite, $GRCO$.

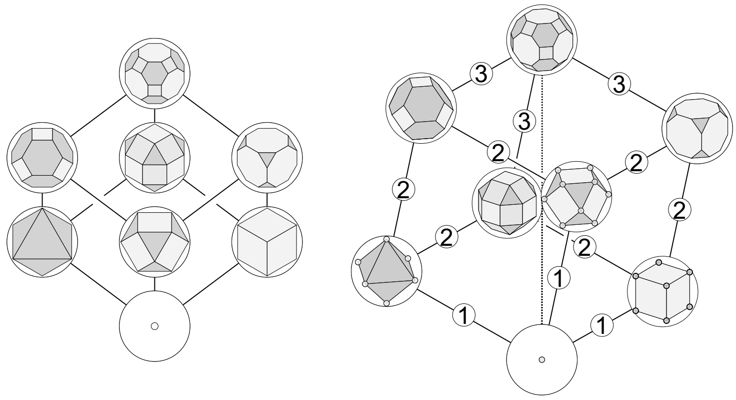

(Reading from bottom to top):
3: $GRCO$.
2: $TC/SRCO/TO$, ↑ to
1: $OH/CO/CB$, ↑ to
0: VP, ↑ to

Fig. 6: (left) Class II rhombic bi-hierarchical network of PPs (view +ve axis); (right) Class II VP—$GRCO$ principal √3 axis. Both sub-figures show the stepped vertical progression of PP pairs.

Thus (restoring gravity), considering the $GRCO$—VP diagonal as the unique vertical primary axis to the schema, each PP provides a locus of realization and/or generation of its neighboring PPs, allowing the 8 PPs of each class to then be ranked according to their pattern of relationship to their adjoining PPs. VP is unique; in step 1 it generates 3 equivalent PPs: $VP \rightarrow OH$, CO, and CB. In step 2, OH, CO, and CB each generate two PPs, i.e., $OH \rightarrow SRCO$ and TO; $CO \rightarrow TO$ and TC; and $CB \rightarrow TC$ and $SRCO$. In step 3, the equivalent TC, $SRCO$, and TO each generate the also unique $GRCO$: TC, $SRCO$, and $TO \rightarrow GRCO$, to culminate the vertical progression. The constant feature of each step is the separation of the faces of one gender (−, 0, +) by unit distance, indicating its driving characteristic.

The schema therefore displays clear stratification (that of the polar zonahedron [12] of the cube), as each PP is generated from, and/or develops into, its fellow PPs. Here, VT only generates; while $GRCO$ is only generated. Four strata (S) of elements are thus evident, of 1 3-fold generator, 3 1-generated and 2 generating; 2 generated and 1 generating; and 1 3-fold generated: $S1$: VP; $S2$: OH, CO, and CB; $S3$: TC, $SRCO$, and TO; and $S4$: $GRCO$, while the schema morphology exhibits clear 3-fold order about the principal VP—$GRCO$ √3 axis. Each of the 5 Classes I−V of regular and semi-regular polytopes according to symmetry is thus characterized by a development sheath of sequences from VP to GR of 3-fold nature, with the PPs of that class disposed in those 4 strata.

For each of the five classes, any constituent PP within that class can be developed by the separation of −ve, neutral, or +ve faces from the source VP in a sequence of steps, so: 0 step: VP; 1 step: PL^+, QR, PL^-; 2 steps: TP^-, SR, TP^+; 3 steps: GR (Fig. 7b). The variations in steps to realize a particular PP by the process of separation of adjoining surface polytopes separating to adjacent surface polytopes by unit distance is therefore: 'no way': VP; one way: PL^+, QR, PL^-; two ways: TP^-, $SRQR$, TP^+; and six ways: $GRQR$.

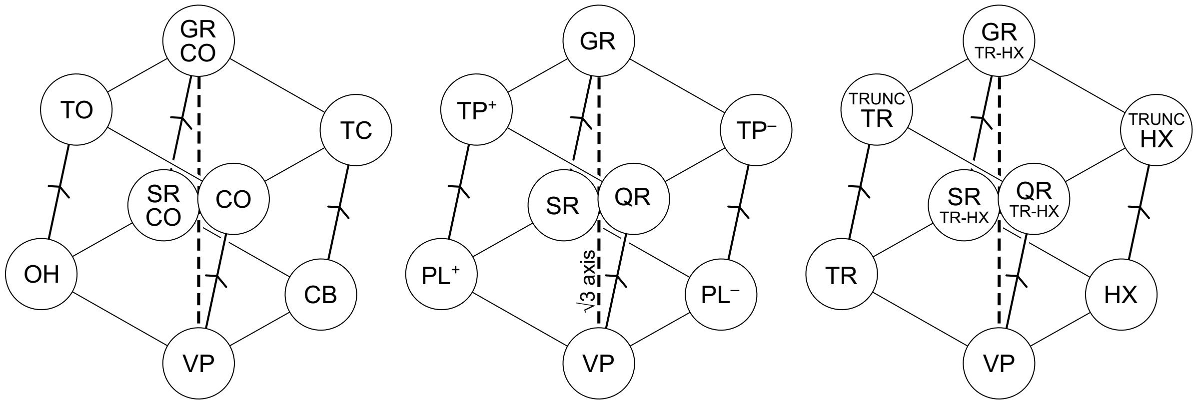

Fig. 7: The pairing of polytopes by neutral faces and their separation showing the 3-fold order: (a) for Class II, (b) Generic, i.e., for all 5 classes of symmetry, and (c) for Class IV.

For Class II as exemplar, this is 0 step/no way, VP_{II}; 1 step/1 way, OH, CO, CB; 2 steps/2 ways, TC, $SRCO$, TO; 3 steps/6 ways, $GRCO$ (Fig. 7a). For Class IV as exemplar, this is 0 steps/no way, VP_{IV}; 1 step/1 way, TR, $QR\ TR{:}HX$, HX; 2 steps/2 ways, $TrncHX$, $SR\ TR{:}HX$, $TrncTR$; 3 steps/6 ways), $GR\ TR{:}HX$ (Fig. 7c). (Alternatively, subduction sequences of the convergence of faces would consist of $GR \rightarrow (TP^+, SR, TP^-) \rightarrow (PL^+, QR, PL^-) \rightarrow VP$). Each family of polytopes therefore demonstrates a high degree of order, and should not be considered accidentally related; or within any one class, by assuming any one PP to be equivalent to the other seven. Rather, they simultaneously crystallize into formal existence as regularly varied concretizations of a profound natural spatial order.

As previously observed, the 3-fold morphology of the 8 PPs in each class is the structure of a polar zonahedron, as also evident in the evolution/involution of the 2D polar zonagon schema of from above or from below. This polar zonagonal geometry at higher frequency (f = (12, 24, 48, 60…) is widely used in traditional Islamic sacred architecture of the dome, in its 3D form and in its 2D surface decoration, as explored in part of my PhD [12:pp.9−34], and offers very real advantages to construction and decoration (equal subdivision of angle in plan; equal length edges; constant vertical gain of edges, so constant slope; corresponding equal vertical stratification of nodes; and nodes lying on a rotated sine wave surface about the principal vertical axis). In sacred and traditional architecture, the form eloquently symbolizes the geometry of the center, projected into time and space; the cycle of manifestation and transformation of a central epiphany emanating from the source, extending to maximum realization in the phenomenal; then reflecting, clarifying, and centering, for the manifestation to be reabsorbed through the center, to return to the noumenal beyond creation.

However, the three-fold symmetry of −ve, neutral, and +ve remains in a sense imperfect, as the duality of the polyhedra intrudes, indicating that the morphology of the neutral differs in kind from that of the polar; a creative tension exists between this characterization and the unfolding of order from the wrapping around of a central axis, to reflective planar symmetry about a central vertical axis of neutrality, as if the sheath of the schema splits open to uncurl to dispose elements and relationships into bilateral symmetry of vertical qualitative differentiation, and horizontal duality/polarity. Hence the subtlety of the 2.5D schema that can mediate that creative tension.

Table IV. Source to goal progression of PTs by the generic separation of one set of (−ve, neutral, or +ve) facial pairs of PPs together with the associated morphological changes of the other two sets of facial polytopes (Fs).

Separating facial PTs	Primary Polytope (PP) transition	Source facial PTs	Goal facial PTs	Source facial PTs	Goal facial PTs
Negative facial PT separation		Neutral facial PT projection		Positive facial PT expansion	
F_0^-	$VP \to PL^+$	${}_0V_0^0$	${}_0E_\alpha^0$	${}_0V_0^+$	${}_0F_\alpha^+$
F_α^-	$PL^- \to SRQR$	${}_0E_\beta^0$	${}_0F_2^0$	${}_1V_0^+$	${}_1F_\alpha^+$
F_β^-	$QR \to TP^+$	${}_1V_0^0$	${}_1E_\alpha^0$	${}_0F_\beta^+$	${}_0F_2^+$
F_2^-	$TP^- \to GRQR$	${}_1E_\beta^0$	${}_1F_2^0$	${}_1F_\beta^+$	${}_1F_2^+$
Neutral facial PT separation		Positive facial PT expansion		Negative facial PT expansion	
F_0^0	$VP \to QR$	${}_0V_0^+$	${}_0F_\beta^+$	${}_0V_0^-$	${}_0F_\beta^-$
F_α^0	$PL^+ \to TP^+$	${}_0F_\alpha^+$	${}_0F_2^+$	${}_1V_0^-$	${}_1F_\beta^-$
F_β^0	$PL^- \to TP^-$	${}_1V_0^+$	${}_1F_\beta^+$	${}_0F_\alpha^-$	${}_0F_2^-$
F_2^0	$SRQR \to GRQR$	${}_1F_\alpha^+$	${}_1F_2^+$	${}_1F_\alpha^-$	${}_1F_2^-$
Positive facial PT separation		Negative facial PT expansion		Neutral facial PT projection	
F_0^+	$VP \to PL^-$	${}_0V_0^-$	${}_0F_\alpha^-$	${}_0V_0^0$	${}_0E_\beta^0$
F_α^+	$PL^+ \to SRQR$	${}_1V_0^-$	${}_1F_\alpha^-$	${}_0E_\alpha^0$	${}_0F_2^0$
F_β^+	$QR \to TP^-$	${}_0F_\beta^-$	${}_0F_2^-$	${}_1V_0^0$	${}_1E_\beta^0$
F_2^+	$TP^+ \to GRQR$	${}_1F_\beta^-$	${}_1F_2^-$	${}_1E_\alpha^0$	${}_1F_2^0$

These correspondences between classes of the various facial transformations of separation, morphing/expansion of the −ve or +ve faces or extrusion/projection of the neutral faces help validate the 2.5D schema and the rhombic schema of the evolution of faces, while serving to characterize the progressions and interrelationships of the polyhedra and tessellations.

In accord with the rhombic schema of Fig. 3, faces are thus null (level 0), regular or quasi-regular (i.e., of the regular or quasi-regular PT; level 1), or double (level 2); i.e., only ever (0, α or β, or 2):

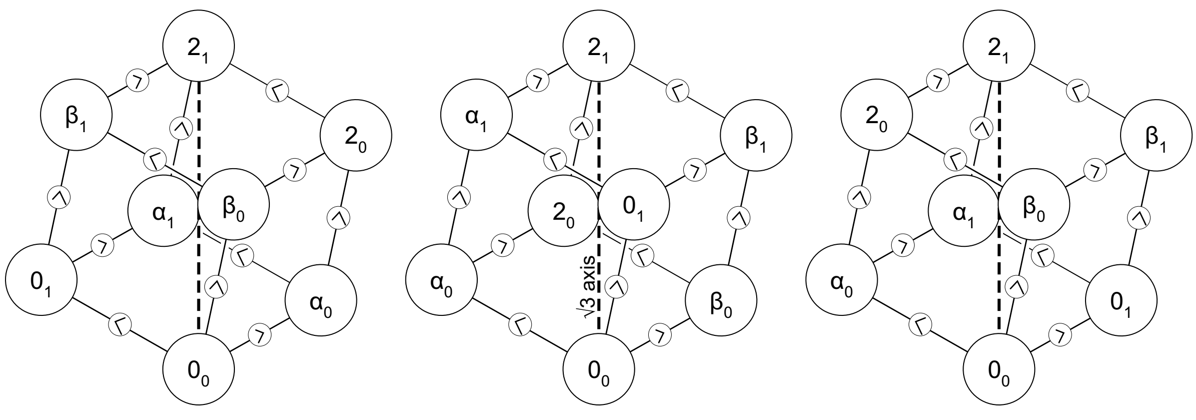

A. Negative faces
Z- and X-axes:
Front right: 0→α|β→2 rhomb d=0
Back left: 0→α|β→2 rhomb d=1
Y-axis: Separation of −ve faces
(bold) d=0 → d=1

B. Neutral faces
X- and Y-axes:
Lower: 0→α|β→2 rhomb d=0
Upper: 0→α|β→2 rhomb d=1
Z-axis: Separation of ntrl faces
(bold) d=0 → d=1

C. Positive faces
Y- and Z-axes:
Front left: 0→α|β→2 rhomb d=0
Back right: 0→α|β→2 rhomb d=1
X-axis: Separation of +ve faces
(bold) d=0 → d=1

Fig. 8: Formal transformations for (L to R) −ve, ntrl, and +ve clusters of the faces of Fig. 1 of the cubic schema show that the patterns of separation and morphing/extrusion are identical across faces, with −ve | +ve reflective.

F = Face, including where relevant (on axis) null or degenerate 0D *VT* and 1D *E*, as well as 2D polygons.

Right superscript: Polarity, of –, negative; 0, neutral; or +, positive.

Left subscript: Spacing of faces of d=0 : adjoining, or d=1 : adjacent, with 1 = edge length of polytope.

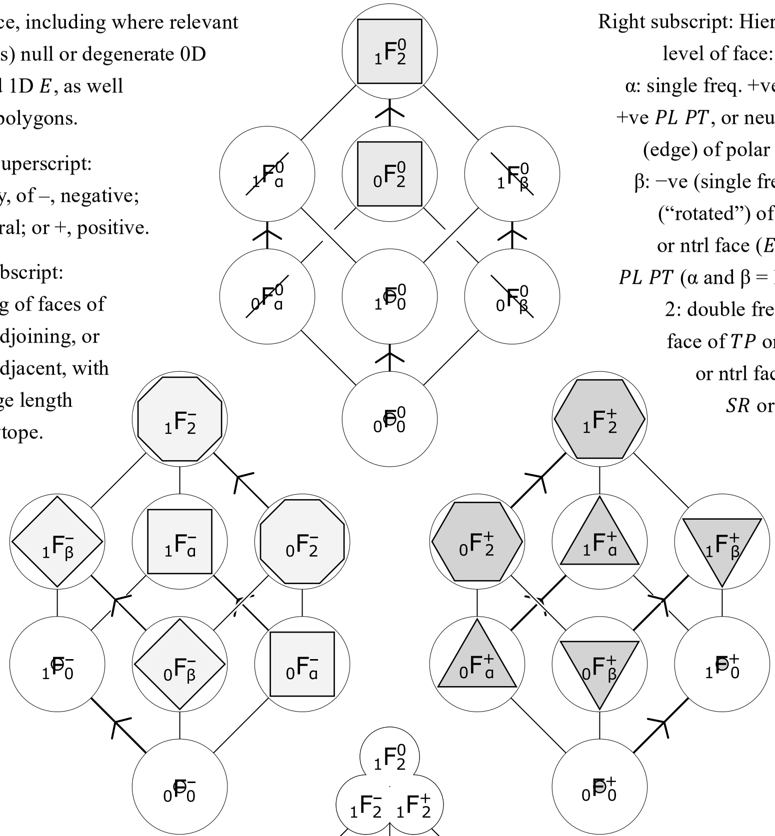

Right subscript: Hierarchical level of face: 0 = *VT*; α: single freq. +ve face of +ve *PL PT*, or neutral face (edge) of polar +ve *PT*; β: −ve (single freq.) face ("rotated") of *QR PT*, or ntrl face (*E*) of −ve *PL PT* (α and β = level 1); 2: double freq. −|+ve face of *TP* or *GR PT* or ntrl face/*SQ* of *SR* or *GR PT*.

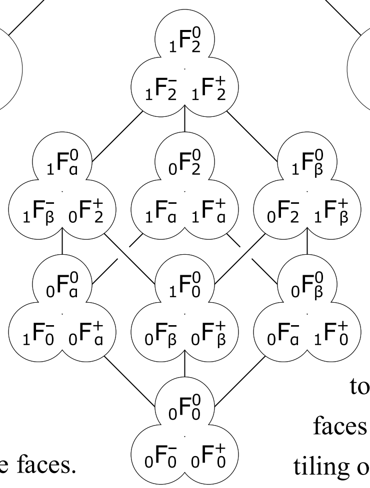

Fig. 9: Generic 2.5D Schema of faces across classes, with exemplar Class II faces:
Upper: ntrl faces.
Left: −ve faces.
Right: +ve faces.
Lower: ntrl, −ve, and +ve faces.

Letting faces be null on-axis 0D vertices or 1D edges enables formal consistency across the *PP*s. Taken together, ntrl, −ve, and +ve faces form each polyhedron or tiling of the 5 symmetry classes.

F = Face, including where relevant (on axis) null or degenerate 0D *VT* and 1D *E*, as well as 2D polygons.

Right superscript: Polarity, of –, negative; 0, neutral; or +, positive.

Left subscript: Spacing of faces of d=0 : adjoining, or d=1 : adjacent, with 1 = edge length of polytope.

Right subscript: Hierarchical level of face: 0 = *VT*; α: single freq. +ve face of +ve *PL PT*, or neutral face (edge) of polar +ve *PT*; β: −ve (single freq.) face ("rotated") of *QR PT*, or ntrl face (*E*) of −ve *PL PT* (α and β = level 1); 2: double freq. −|+ve face of *TP* or *GR PT* or ntrl face/*SQ* of *SR* or *GR PT*.

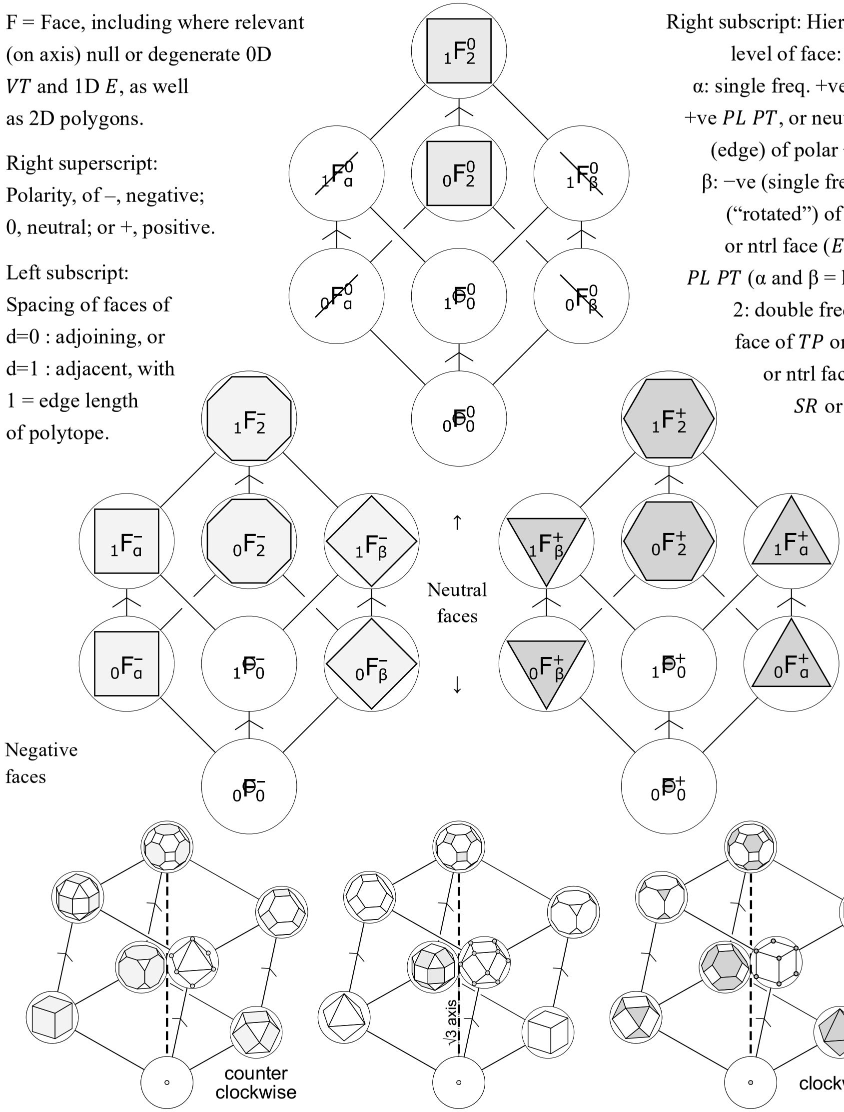

Fig. 10: Rotated Class II 2.5D Schema of faces: top/center: ntrl; left: −ve faces (−2π/3); right: +ve faces (+2π/3). −ve/ntrl/+ve faces combine to form each *PT*.

5. Integrating the relationships

The formal structure or structural morphology of the elements of the five classes of regular and semiregular polyhedra and tessellations, and the relationships between the elements in any one class, thus become clear. The key to this morphology consists of the 2.5D cubic schema together with the rhombic schema of the development of faces, the reorientation of the cube on its √3 long vertical principal axis of VP—GR, and recognition of the separation of faces characterizing any one of the cubic schema links between polytopes as bundles/sheaths of parallel faces of the cube as zonahedron. Either of the other 2 sets of characteristics of the simultaneous morphing or expansion of +ve or −ve facial polytopes, and the projection or extrusion of neutral facial polytopes, can then be recognized as the other 2 zonahedral bundles of the zonahedral cube, respectively, notwithstanding these are not simply equivalent to the neutral case that exploits the primary orthogonal axes of the rhomb, but are differentiated into pairs of pairs that exploit the inclined axes/opposite edges of the rhomb, separating the d=0 and 1 rhombs.

In the negative facial case (Fig. 8A), −ve front right cubic schema faces are adjoining d=0, while back left are adjacent d=1. On the Z-axis, the pairs of pairs are 2×(0→β) and 2×(α→2), where d=0: (0_0→β_0) and (α_0→2_0), and d=1: (0_1→β_1) and (α_1→2_1). On the X-axis, the pairs of pairs are 2×(0→α) and 2×(β→2), where d=0: (0_0→α_0) and (β_0→2_0), d=1: (0_1→α_1) and (β_1→2_1).

In the neutral facial case (Fig. 8B), neutral lower cubic schema faces are adjoining d=0, while upper are adjacent d=1. On the X-axis, the pairs of pairs are 2×(0→β) and 2×(α→2), where d=0: (0_0→β_0) and (α_0→2_0), and d=1: (0_1→β_1) and (α_1→2_1). On the Y-axis, the pairs of pairs are 2×(0→α) and 2×(β→2), where d=0: (0_0→α_0) and (β_0→2_0), d=1: (0_1→α_1) and (β_1→2_1).

In the positive facial case (Fig. 8C), +ve front left cubic schema faces are adjoining d=0, while back right are adjacent d=1. On the Y-axis, the pairs of pairs are 2×(0→α) and 2×(β→2), where d=0: (0_0→α_0) and (β_0→2_0), and d=1: (0_1→α_1) and (β_1→2_1). On the Z-axis, the pairs of pairs are 2×(0→β) and 2×(α→2), where d=0: (0_0→β_0) and (α_0→2_0), d=1: (0_1→β_1) and (α_1→2_1).

In each case of −ve, ntrl, and +ve clusters of faces, the separation of faces by gender is represented as the Y–, Z–, or X–axis separating rhombic schema of 0→α|β→2 for d=0 → d=1.

Generically, for any class, and for each case of −ve, neutral, or +ve facial polytope, each constituent PP can be uniquely described in terms of two parameters: 1. The level of facial polytope evolution, i.e., (0, α | β, 2), and 2. the separation of facial polytope distance, whether adjoining or adjacent, i.e., (0, 1). The PPs can therefore be tabulated according to their facial evolution and separation:

Table V. Generic expressions of facial evolution and separation of the constituent PPs of each class.

Sep. of faces	Negative				Neutral				Positive			
d	0	α	β	2	0	α	β	2	0	α	β	2
0	VP	PL^-	QR	TP^-	VP	PL^+	PL^-	SR	VP	PL^+	QR	TP^+
1	PL^+	SR	TP^+	GR	QR	TP^+	TP^-	GR	PL^-	SR	TP^-	GR

Any specific case: −ve, neutral, or +ve of the facial polytope, in combination with the separation (Sep.) of those neighboring facial polytopes of adjoining (d=0) or adjacent (d=1), is sufficient information to determine the PP of that class, whether VP, $PL^{-/+}$, QR/SR, $TP^{-/+}$, or GR. Excepting the QR/SR pair, the −ve and +ve cases are reflectively symmetric about the VP—GR axis, while the neutral case shows different structure, which suggests that my neutral annotation and analysis might need revision. The overall structure indicates that in addition to the obvious $PL^{-/+}$ and $TP^{-/+}$ polarities, there is a limited QR/SR polarity, as there is comprehensive VP/GR polarity—of potential–realization, of noumenal–phenomenal, of 'beyond creation'–being.

Generically, for any class, and for each case of −ve, neutral, or +ve facial polytope, each constituent PP can alternatively be uniquely described according to its property of gendered −ve, neutral, and/or +ve facial separation, hence $\mathrm{d}_{-0+} = 0$ or 1:

Table VI. The constituent PPs of each class as generic expressions of facial separation quality d= |−0+|.

Generic

	GR	
TP^+	SR	TP^-
PL^+	QR	PL^-
	VP	

Facial separation d

	$\|111\|$	
$\|110\|$	$\|101\|$	$\|011\|$
$\|100\|$	$\|010\|$	$\|001\|$
	$\|000\|$	

Class II

	$GRCO$	
TO	$SRCO$	TC
OH	CO	CB
	VP	

This returns the tentative 3-fold order to bilateral symmetry, and the historical perspective of the perfection of the regular PLs, though elsewhere I make the alternative case that it is the QRs that are perfect, while the PLs are extremes [13]. But given that these polyhedra and tessellations are discovered as projections of the noumenal (ideal) into the phenomenal (contingent) realm, the enigmatic possibility remains that such limited 3-fold symmetry represents a trace of primordial evolution of formal symmetry, suggesting that the constraints and properties of space that we encounter might at the cosmic level be subject to change, and raising the intriguing question of whether such change would (or could only) be abrupt or gradual. One might speculate whether in our cosmos, three-fold symmetry is unstable (e.g., is it common in the animal kingdom? It seems at least uncommon); and to be subsumed into a kind of 2-step bilateral symmetry that I address in a subsequent paper, which is characterized by complementary forms as (−ve ↔ +ve) (in their pure form, dual), rather than identical, allowing the tentative self-reflective quality of the neutral ($VP \leftrightarrow GR$ and $QR \leftrightarrow SR$)). Further, do these patterns and their harmonic order correlate with quantum forms and field behavior, where resonance seems fundamental?

6. Conclusion

Earlier intuition [11, 12] indicated that the elegance of the regular and semiregular polyhedra and tessellations must surely be matched by their order, and has inspired my subsequent research.

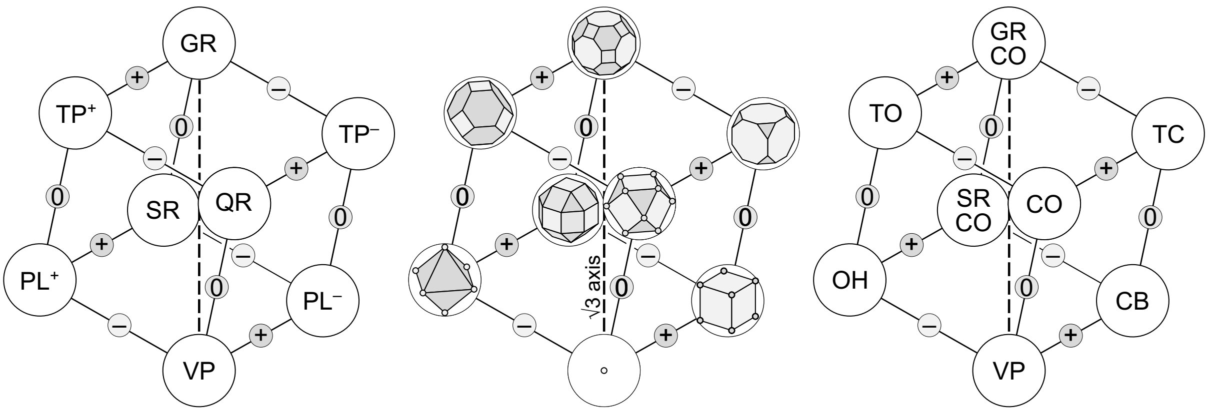

Fig. 11: Separation of faces by −ve/ntrl/+ve gender. Each transition $PP_0 \rightarrow PP_1$ is characterized by a separation of neighboring faces from adjoining (d=0) to adjacent (d=1), in 3 X,Y,Z zones. Left to right: Generic, Class II polytopes, and IDs. PPs evolve (devolve) upwards (downwards) $VP \rightarrow GR$ ($GR \rightarrow VP$).

In response, Fig. 11 shows that any PP transition $PP_0 \rightarrow PP_1$ is characterized by a separation of neighboring faces from adjoining (d=0) to adjacent (d=1), in one of the 3 X, Y, or Z zones.

Dashed arrows show +ve, neutral, and −ve views for Fig. 11.

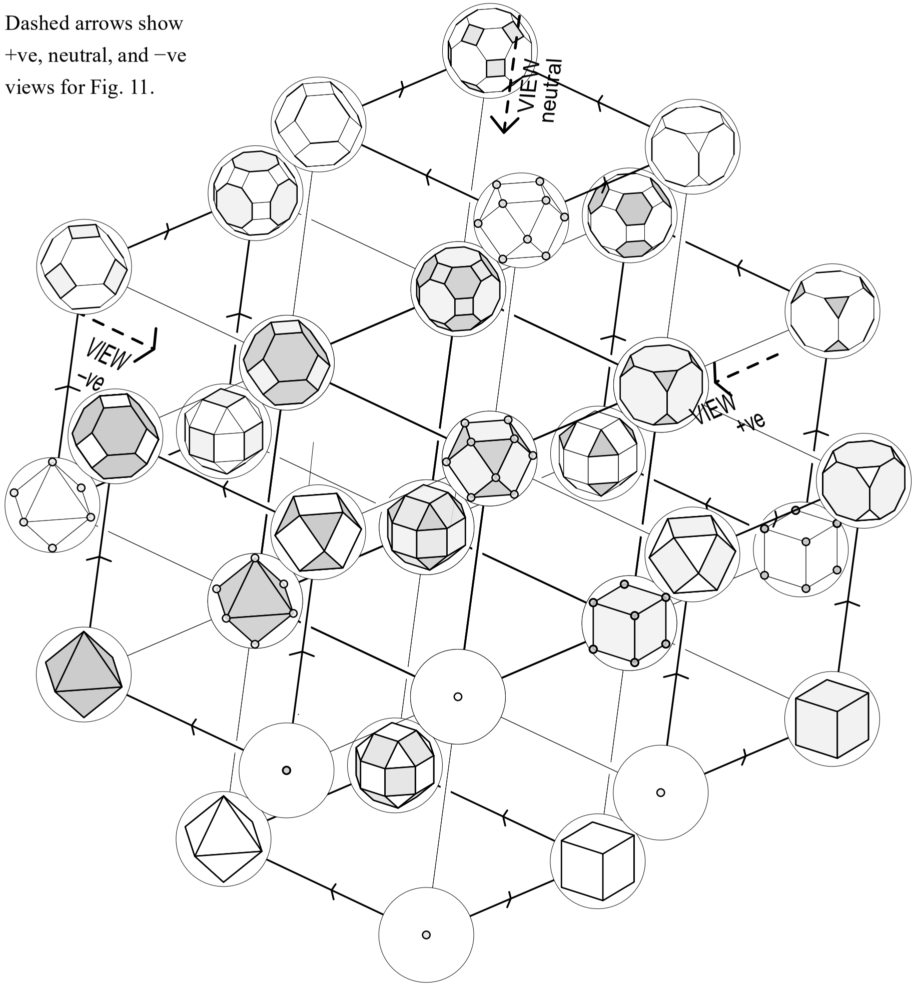

Fig. 12: Expansion of 2.5D cubic schema to demonstrate the rhombic schema on each of its 6 faces. Lower left, bottom, and lower right outermost faces show +ve, ntrl, and −ve (d=0) adjoining rhombic schema; upper right, top, and upper left outermost faces show +ve, ntrl, and −ve (d=1) adjacent rhombic schema.

In each cluster of Fig. 12, lower rhomb is of adjoining faces (d=0) of the polytope, upper rhomb is of the corresponding adjacent faces (d=1). Vertical links indicate these corresponding pairs. Each rotated rhomb traces the same progression of $< 0 \rightarrow \alpha|\beta \rightarrow 2 >$ of lower level 0-polytope, level 1 α and β polyhedra, and level 2 polyhedra. The −ve and ntrl clusters show α at left, while +ve shows β at left. Note the subtle “circulation” of polyhedra at the mid-levels from cluster to cluster; only the ntrl shows the initial schema, while the +ve and −ve are rotated. These clusters correspond to those of Fig. 8, so the −ve schema (cluster) is rotated counter-clockwise ($-2\pi/3$) from the ntrl schema (cluster) about the vertical GR—VP main $\sqrt{3}$ axis, while the +ve schema is rotated clockwise ($+2\pi/3$); bear in mind that in this figure, the polyhedra of the schema rotate (as a group), while their relationships (the schema edges) are conserved through the three states of −ve, ntrl, and +ve.

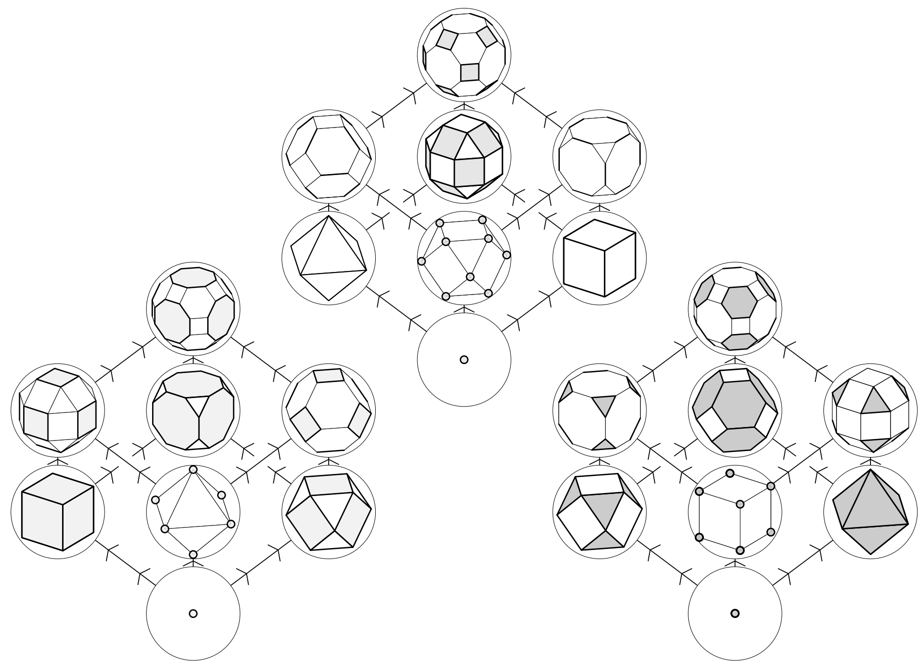

Fig. 13: Bi-rhombic schema for the −ve (left), ntrl (center), and +ve (right) faces, abstracted from the outer 6 faces of the extended 2.5D schema in the previous figure. For consistency, 3 views are taken through the cube, one per cluster, from (outside) adjacent (d=1) to (inside) adjoining (d=0) faces.

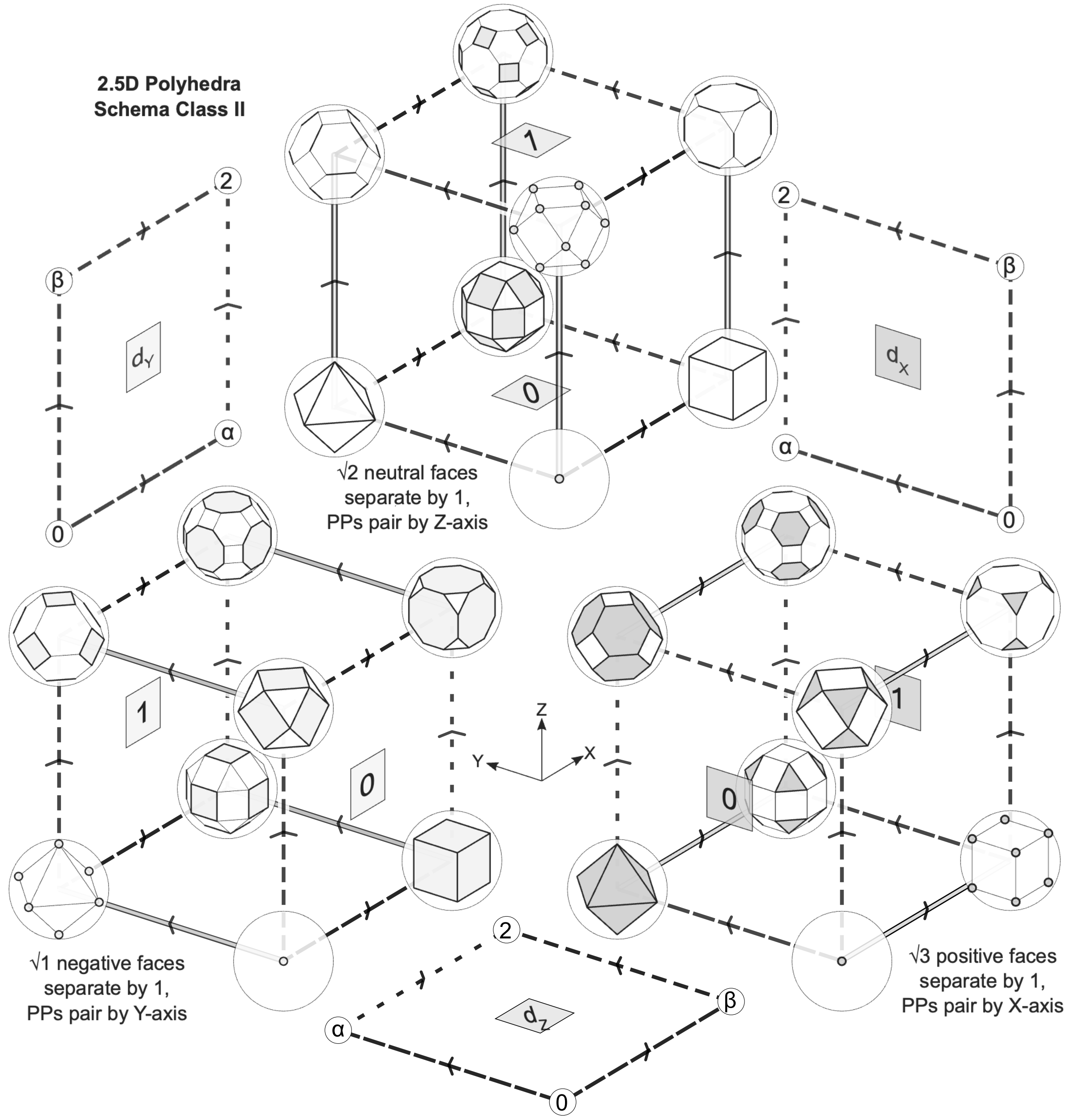

Fig. 14: The simultaneous various facial evolutions that apply. Double black lines of rising left, vertical, and rising right denote the separation of faces for the respective −ve Y, ntrl Z, +ve X (lower left, top, lower right) axes. Single black lines of varied dash denote the simultaneous evolution of faces of two paired (0→α) and (α→2), and (0→β) and (β→2), with *PP* faces colored light grey, mid-grey, dark grey, respectively, where (0→α|β) lines are long close dashes, while (α|β→2) lines are short far dashes. In each schematic cube, the 4 −ve, ntrl, or +ve parallel lines denoting the evolution of faces correspond to the bundles of edges of the three zones of the cubic zonahedron. The double line zonal bundle separates the two faces of the schematic cube as enantiomorph of the rhombic schema, the polytopes of one face for d=0 where faces are adjoining (sharing a common vertex or edge), while those of the opposing face for d=1 where the faces are adjacent (separated by unit distance). The −ve, ntrl, +ve rhombs for the Y, Z, X axes are abstracted at top left, bottom, top right, respectively. All 3 cubic schema apply simultaneously; the −ve and +ve cubic schema are bilaterally symmetric, the transformations of the schema applying to the relationships (edges), not the *PP* s. All five classes demonstrate the same morphology, allowing for the dimensional difference between the polyhedra and the polygonal tessellations (Classes I–III *cf.* IV and V).

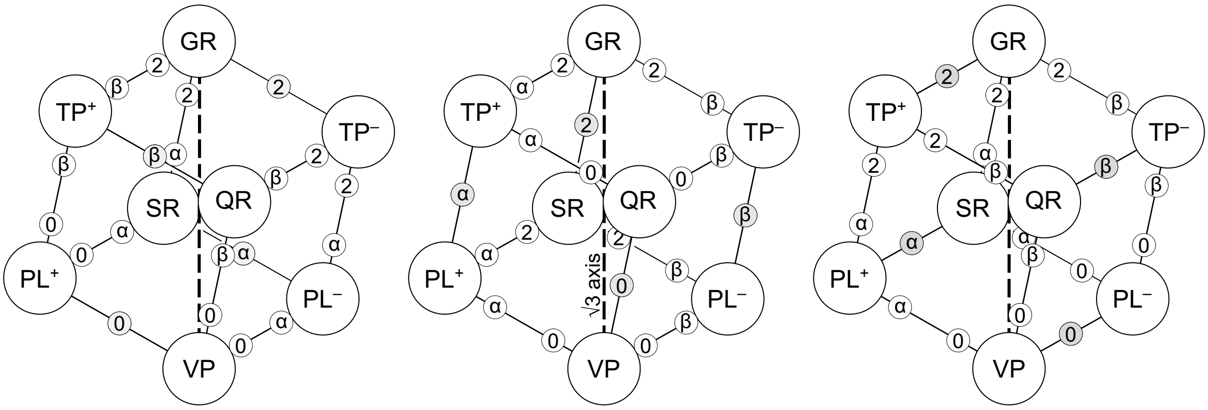

Fig. 15: Simultaneous transformation of faces by (0→α|β→2) evolution. As faces of one −ve/ntrl/+ve gender separate, faces of the remaining two genders transform, in pairs of transitions of PPs of each zone. Quartiles show facial evolutionary stage, with zones in (0→α, β→2) or (0→β, α→2) pairs. Mid-points conserve facial separation, each zone with 1 (0, α, β, 2) face. Left to right: −ve; ntrl; +ve faces.

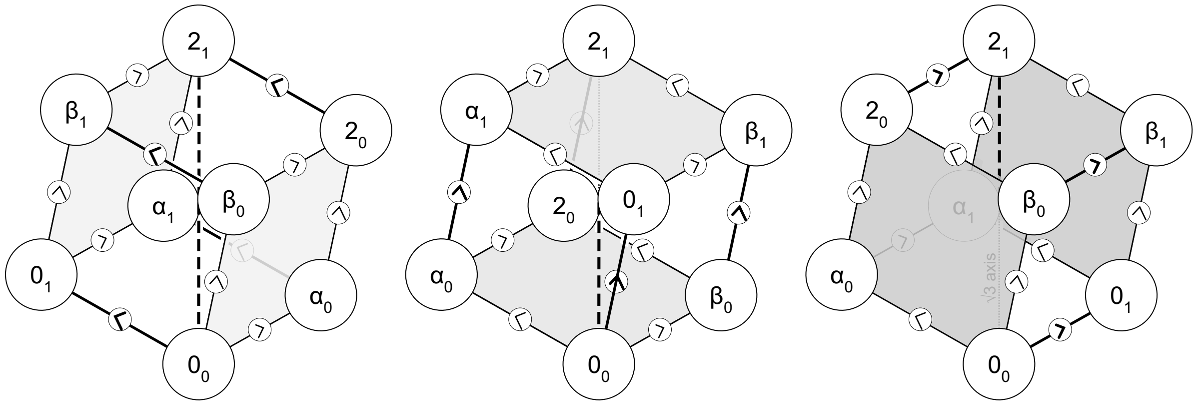

Fig. 16. Y, Z, and X zone separation of the d=0 and d=1 rhombic schema of −ve, ntrl, +ve faces (left to right).

Figure 15 demonstrates that for each case of −ve, ntrl, and +ve faces, as one zone of the cubic schema represents the separation of −ve, ntrl, or +ve faces, respectively, one of the other two zones represents two pairs of parallel 0→α and β→2 transitions, while the other zone represents two pairs of parallel 0→β and α→2 transitions. Figure 16 shows that for each case of −ve, ntrl, and +ve faces, the X, Y, or Z axial zone of separation of faces representing 0→0, α→α, β→β, and 2→2 of the cubic schema of d=0 and d=1, respectively, separates two corresponding rhombic schema 0 → α|β → 2 of d=0 and d=1, respectively, as Fig. 8 has previously shown.

Hence the separation of faces appears fundamental to the progression of PPs represented by the edges of the cubic schema, the SOF for one gender being complemented by the simultaneous morphing of the faces of the other two genders according to either of two opposite edges of the rhombic schema of (0→α and β→2), or (0→β and α→2), respectively.

This elegant morphology characterizes the order of the regular and semi-regular polyhedra and tessellations. Consequent upon the assumption of a null polytope in each of the five symmetry classes, and of degenerate 0D and 1D facial polytopes of certain vertices and edges by gender; the cubic schema of PPs; its rotation to the vertical VP→GR √3 axis; the rhombic schema enantiomorphs of null 0, regular α or quasi-regular β, and $2f$ faces; the limited 3-fold symmetry to the order; the fundamental separation of faces d=0 to 1; and the transitional form of the snub enantiomorphs of each class at the center of the cubic schema, at the mid-point of the $SRQR$—QR jitterbug and main VP—GR axes, the typology of the polyhedra and tessellations is hereby adequately described.

This work might find application in polyhedral geometry, crystallography, chemistry (phase transitions, bi-polymers, smart polymers, catalysts), artificial bone matrix (integrating variable flexibility), biomedicine (triggered deployment of dosage of drug from nanocages), smart material, wearable (conformable) electronics, space structures (dynamic structures, deployable antennae in Space), nanostructures, perhaps quantum mechanics and field theory, and potentially, insights into the nature of space itself. Future research is intended to refine the order of the all-space-filling periodic arrays of 2D and 3D PTs in the light of this cubic schema.

Historically, the regular (and semi-regular) polyhedra as independent entities have been recognized as perfect (and semi-perfect) forms. However, while such formal perfection should at the very least be matched in their overall structure and morphology, I am unaware of any adequate order having previously been advanced. This paper redresses that shortfall with reference to the separation of one set of +ve, ntrl, or −ve faces characterizing the zonahedral progression of PP_1 to PP_2 on the rotated 2.5D cubic schema, while the other two sets of faces evolve according to the rhombic schema. It has been a privilege to glimpse such rare perfection.

References

[1] K. Critchlow, Order in Space. Thames and Hudson, London, 1969.

[2] B. Grünbaum and G. C. Shephard, Tilings and Patterns. W. H. Freeman, New York, 1987.

[3] R. C. Meurant, A Novel 2.5D Schema of the Regular and Semi-regular Polytopes and their Sequences, with Analysis by Polytope and Surface Elements. Information Journal, International Information Institute, Vol.24, No.2, June 2021, pp.51–64. PDF 68.

[4] R. C. Meurant, A New 2.5D Schema of the Regular and Semi-regular Polyhedra and Tilings: Classes II and IV. *Information*, L. Li, R. Ashino, and C.-C. Hung (eds.), Proceedings of The Tenth International Conference on Information, Tokyo/Zoom, Mar. 6–7, 2021, 29–34. PDF 67.

[5] R. C. Meurant, Towards a New Order of the Polyhedral Honeycombs: Part III: The Developed Metaorder, Form and Counterform. *Information*, Vol.22, No.1, Jan. 2019, 23–45. PDF 66.

[6] R. C. Meurant, Form and Counterform in the Periodic Polyhedral Honeycombs. Information 2018: L. Li et al. (eds.), Proc. of The 9th Int. Conf. on Information, Tokyo, Dec. 7–9, 2018, 51–56. PDF 65.

[7] R. C. Meurant, Expansion Sequences and their Clusters of the All Space-filling Periodic Polyhedral Honeycombs. *Information*, Vol.20, No.10(A), Oct. 2017, 7345–7362. PDF 64.

[8] R. C. Meurant, Sequences of the All Space-filling Periodic Polyhedral Honeycombs. Information 2017. L. Li et al. (eds.), Proceedings of The Eighth International Conference on Information, Tokyo, May 17–18, 2017, 151–154. PDF 63.

[9] R. C. Meurant, Towards a Meta-Order of the All-Space-Filling Polyhedral Honeycombs through the Mating of Primary Polyhedra. *Information*, Vol.19, No. 6(B), June 2016, 2111–2124. PDF 62.

[10] R. C. Meurant, Towards a New Order of the Polyhedral Honeycombs: Part II: Who Dances with Whom? Information 2015: L. Li and T.-W. Kuo (eds.), Proceedings of The Seventh International Conference on Information, Taipei, Nov. 25–28, 2015, 369–373. PDF 61.

[11] R. C. Meurant, A New Order in Space – Aspects of a Three-fold Ordering of the Fundamental Symmetries of Empirical Space, as evidenced in the Platonic and Archimedean Polyhedra – Together with a Two-fold Extension of the Order to include the Regular and Semi-regular Tilings of the Planar Surface. *Int. J. of Space Structures*, Vol.6 No.1, Univ. of Surrey, Essex, 1991, 11–32. PDF 06.

[12] R. C. Meurant, The Aesthetics of the Sacred: A Harmonic Geometry of Consciousness and Philosophy of Sacred Architecture (3rd ed.), The Opoutere Press 1989 ISBN 0-908809-02-6. (PhD thesis, Univ. of Auckland, 1984). Available from the author, see http://www.rmeurant.com/its/books.html

[13] R. C. Meurant, The Myth of Perfection of the Platonic Solids. People and Physical Environment Research PAPER Conference on Myth Architecture History Writing, University of Auckland, New Zealand, July 1991. PDF 07.

Supplementary Information: References [3−11, 13] as PDFs (68−61, 06, 07), and PDF 71 of this paper, in color or greyscale, are available at http://www.rmeurant.com/its/papers/polygon-1.html

Nomenclature: NON-DIMENSIONAL: –ve, negative; ntrl, neutral; +ve, positive; f, frequency (of F); GR, great rhombic; $L0{-}L2$, level (0, 1= α and β, 2) of rhombic schema; P, pole or polar; $S1{-}4$, strata (1–4) of rotated cubic schema; Snb, snub; SR, small rhombic; $Trnc$, truncated. ● ZERO-DIMENSIONAL: V^0, neutral vertex (NV); V, vertex (but can be 1 or 2D 'F'); VP, verticial polytope hence VP_{I-V}. ● ONE-DIMENSIONAL: d, distance of proximal Fs (0 or 1); E, edge (EG) but here can be 2D 'F'; E^0, neutral edge (NE) but here 2D 2-gon 'F'. ● TWO-DIMENSIONAL: DD, dodecagon (12-gon); HX, hexagon or hexagonal array; OG, octagon; PR, polar polygon; RH, rotated hexagon; RP, 'rotated' polar polygon (trunc.); RS, 'rotated' (trunc.) square; RT, 'rotated' (trunc.) triangle; RX, 'rotated' (trunc.) hexagon; SQ, square; SQ^0, neutral square (NS); $SQ{:}SQ$, square–square array; TP, truncated polar polygon ($2f$); TR, triangle or triangular array; $TR{:}HX$, tri-hex array; $TrncHX$, truncated hexagonal array; $TrncTR$, truncated triagonal array; ZG, zonagon. ● THREE-DIMENSIONAL: CB, cube; CO, cuboctahedron; DC, dodecahedron; $GRCO$, great rhombic cuboctahedron; IC, icosahedron; $IC{:}DC$, icosidodecahedron; OH, octahedron; $OH{:}CB$, octahexahedron (= CO); $SnbCO$, snub cuboctahedron; $SRCO$, small rhombic cuboctahedron; TC, truncated cube; TD, truncated dodecahedron; TH, tetrahedron; $TH{:}TH$, tetra-tetrahedron (Class I colored OH); TI, truncated icosahedron; TO, truncated octahedron; TP, truncated polar polytope; TT, truncated tetrahedron; ZH, zonahedron. ● MULTI-DIMENSIONAL: F, face = facial PT (in this paper, 0D, 1D, or 2D); α, regular facial polytope; β, quasiregular facial polytope; $GRQR$, great rhombic quasiregular; PL, polar polytope; PP, primary polytope; PT, polytope; QR, quasiregular; $SnbQR$, snub quasiregular; $SRQR$, small rhombic quasiregular. ■

Robert C. Meurant □ B.Arch (Hons) (1978), and PhD in Architecture (1984), University of Auckland, New Zealand □ MA in Applied Linguistics (2007), University of New England, Australia □ Director Emeritus, Institute of Traditional Studies □ Taught in universities in New Zealand, the United States, and Korea □ Published 6 books, over 70 papers, presented papers in New Zealand, the U.S., the U.K., Japan, and Korea □ For many years, a director of the Science and Engineering Research Support Society (SERSC), Korea □ Research interests: sacred and traditional geometry, art, and architecture; the traditional philosophy of art; number and form; the polyhedra; structural morphology and geometry; deployable Space habitation and large-scale structures in microgravity, nanoarchitecture, applied linguistics ■
ORCID iD: 0009-0001-4142-0699

This paper revises the author's "*The morphology of the regular and semi-regular polyhedra and tessellations according to the separation of facial polytopes*" (previously published in the European Journal of Applied Sciences Vol. 11, No. 1, Jan. 25, 2023), and is the first in a series of four or more papers to be published in this journal that develop related work. A color PDF of this paper, PDF 71, can be accessed at: http://www.rmeurant.com/its/papers/polygon-1.html.